Proceedings of the 4th International Conference on Environmental Geoscience and Earth Ecology
DOI: 10.54254/2753-8818/2026.34300

Water Purification Initiative: A Wastewater Treatment Solution Based on Zinc Oxide-Enhanced Composite Hydrogel

YunKyung Kwak

Shanghai American School PUXI Campus, Shanghai, China
kellykwak21@icloud.com

Abstract. Clean water scarcity is an urgent global challenge, particularly in regions where untreated textile wastewater is discharged directly into the environment. Textile effluents contain high concentrations of synthetic dyes that pose serious environmental and human health risks. Conventional dye-removal technologies are often limited by low efficiency, strict operational requirements, and secondary sludge generation. To address these challenges, this study develops a low-cost, sustainable, and efficient adsorption-based remediation material based on a zinc oxide nanoparticle-embedded sodium alginate hydrogel (ZnO@SA). ZnO nanoparticles with well-defined rectangular prism morphology were successfully synthesized and incorporated into a sodium alginate matrix via $Ca2^{+}$–induced ionic crosslinking. We employed SEM, TEM, XRD, FTIR, and EDS to analyze the structure and composition. The results verified the formation of high-purity crystalline ZnO and the homogeneous dispersion of nanoparticles throughout the hydrogel network. Compared to the control alginate hydrogel, the ZnO@SA hydrogel exhibited reduced pore size, increased network compactness and viscoelastic stiffness. We assessed the dye adsorption performance by employing methylene blue as a representative textile dye. The results from the UV-Vis spectroscopy indicate that the dye removal capacity of the ZnO@SA hydrogel is significantly enhanced compared to the SA hydrogel. Time-dependent adsorption studies demonstrated sustained dye uptake over multiple days, highlighting the structural stability and prolonged adsorption capability of the composite material. Overall, this study developed a zinc oxide-reinforced sodium alginate composite hydrogel capable of effectively removing dyes from wastewater, offering multiple advantages including cost-effectiveness, biodegradability, and stable mechanical properties. The ZnO@SA composite hydrogel presents a highly promising solution for decentralized and resource-constrained textile wastewater treatment.

Keywords: Zinc oxide, Sodium alginate, Hydrogel, Methylene blue, Wastewater treatment

1. Introduction

Clean water is indispensable for maintaining health, sanitation, and human dignity, yet the global pollution crisis has left millions struggling to access both the quality and quantity of water they need. One major contributor to this crisis is the textile industry, which releases large quantities of synthetic dyes into wastewater. When these dyes are discharged without proper treatment, they

© 2026 The Authors. This is an open access article distributed under the terms of the Creative Commons Attribution License 4.0 (https://creativecommons.org/licenses/by/4.0/).

DOI: 10.54254/2753-8818/2026.34300

severely harm the environment by disrupting aquatic food chains, reducing light penetration necessary for photosynthesis, and killing thousands of marine organisms.

The problem is especially severe because textile mills are often geographically clustered, meaning entire communities are exposed to concentrated pollution over long periods of time. In many of these regions, chronic exposure to contaminated water has been linked to a reduction in life expectancy by approximately 5-10 years, highlighting the long-term human cost of textile wastewater pollution. In addition to environmental damage, exposure to untreated dye-contaminated water can cause serious human health issues, including skin and respiratory disorders, dermatitis, cancer, and other life-threatening diseases [1]. Alarmingly, the textile industry alone is estimated to account for nearly 20% of global industrial wastewater pollution, underscoring the urgent need for effective, scalable treatment solutions.

In general, remediation methods used for dye-contaminated wastewater are chemical and biological. Among these technologies, adsorption is widely considered the most promising, as it offers high efficiency, low cost, and the ability to handle multiple pollutants at once. Recently, use of hydrogel as adsorption materials have drawn a lot of interest due to their high adsorption ability [2]. Among the numerous hydrogels, sodium alginate hydrogels derived from natural materials are widely applied due to their advantages such as biocompatibility and non-toxicity. However, practical applications of sodium alginate hydrogels still face bottlenecks in terms of insufficient adsorption capacity and mechanical properties. In recent years, incorporating nanoparticles into sodium alginate hydrogels has proven to be an effective modification strategy. By selecting suitable nanomaterials for composite formation with sodium alginate hydrogels, composite adsorbents with superior comprehensive properties can be developed.

This study proposes embedding zinc oxide nanoparticles into sodium alginate hydrogels to prepare a wastewater treatment material that combines enhanced adsorption performance with superior mechanical properties. The specific research approach is as follows: First, ZnO nanoparticles were synthesized via hydrothermal precipitation and uniformly dispersed within the sodium alginate matrix through ion cross-linking to produce ZnO@SA composite hydrogels. The structural purity of ZnO nanoparticles and their uniform dispersion within the gel network were verified through SEM, TEM, and other characterization techniques. The microstructure, mechanical properties, and rheological behavior of the composite hydrogel were analyzed. Finally, using methylene blue as a model dye, adsorption experiments evaluated the dye removal performance and sustained adsorption capacity of the ZnO@SA hydrogel. This study aims to develop a low-cost, environmentally friendly, highly efficient, and mechanically stable composite hydrogel material, providing a viable solution for the practical treatment of textile dyeing wastewater.

2. Literature review

2.1. Hydrogel

Hydrogels possess well-defined porous architectures and chemically responsive functional groups, allowing them to efficiently capture metal ions and dyes from wastewater [3]. Jung et al. have prepared lignin incorporated poly (vinyl alcohol) hydrogel for removing cationic dye in waste water. The adsorption capacities of this hydrogel were measured at around 190 mg/g [4]. Whilst the synthetic hydrogel may have great absorption capacities, it releases toxic byproducts. Thus, natural material should be introduced to design hydrogel with the great ability of dye adsorption.

Sodium alginate (SA) is typical of natural polysaccharides and their biodegradability, hydrophilicity, and abundance in nature which are well developed as the matrix materials for

DOI: 10.54254/2753-8818/2026.34300

fabricating hydrogels. In addition, the carboxylate groups (COOH) of SA make it straightforward to modify, allowing it to form chemical complexes with multivalent ions [5]. Ankit Verma prepared a porous hydrogel based on sodium alginate and graphite, which achieved a maximum adsorption capacity of 628.93 mg/g [6]. A sodium alginate/coffee waste hydrogel was developed by Haneen M. Alraddadi and co-workers to serve as an adsorbent for removing both organic and inorganic pollutants from aqueous solutions. Their findings demonstrated that this SA/coffee waste composite hydrogel is more effective in adsorbing dye and heavy metal ions than coffee powder alone [7]. These SA-based adsorbents in water treatment were biocompatible and non-toxic in nature. However, the low adsorption capacity of SA-based adsorbents limits their practical use in cost-effective wastewater treatment systems. Moreover, the mechanical strength, stability and heat resistance of SA hydrogel also restricted their use. Thereby, there is an urgent need and great challenge to develop a SA-based hydrogel with an enhanced adsorption capacity for removing dyes from waste water.

2.2. Nano-reinforcement strategy

Recent studies indicate that selecting and embedding a suitable novel nanoparticle into a hydrogel can lead to both significantly improved dye adsorption capacity and enhanced mechanical properties [8]. Sajjad Hussain prepared a CS/PEG/ZnO composite hydrogel using Zn^{2+} as a cross-linker. He showed that this material is capable of efficiently adsorbing Congo red (CR) dye from water [9]. Zhou has tried adding the magnetic nanoparticle into gelatin hydrogel. The stiffness of composite hydrogel can be adjusted with the addition of nanoparticles [10]. Thus, compositing SA hydrogel with other nanoparticles, further, can increase the adsorption capacities as well as mechanical stability of the SA-based composite hydrogel.

Nanoparticle-based materials have become widely applied in water pollution removal, with titanium dioxide (TiO_2) , silicon dioxide and zinc oxide among the most extensively studied examples [11]. Among metal oxides, zinc oxide (ZnO) are particularly promising due to their large surface area, high surface reactivity, and strong photocatalytic properties. Their specific surface area has been reported to exceed that of several traditional polymeric adsorbents such as chitosan, allowing for greater dye interaction and accelerated degradation [12]. Moreover, ZnO with a bandgap of 3.3 eV that is comparable to the 3.2 eV bandgap of TiO_2, additionally offers higher electron mobility, longer charge-carrier lifetimes, and lower production costs, as well as ease of fabrication into diverse nanostructures. Together, these advantages make ZnO a theoretically attractive candidate for photocatalytic dye removal [13]. Fatemeh Asjadi has synthesized ZnO nanoparticles via a simple hydrothermal method. SEM and XRD analyses showed that the resulting ZnO nanoparticles measured approximately 200 nm in size. At the same time the synthesized ZnO nanoparticles with a surface area of 32.7 m^2/g have been demonstrated to effectively remove methylene blue (MB) dye from an aqueous solution [14]. Given the above circumstances, this study proposes embedding zinc oxide nanoparticles into sodium alginate (SA) hydrogels to obtain a decontamination material with enhanced adsorption capacity and superior mechanical properties.

3. Research methods

3.1. Materials

All chemical reagents are of analytical grade and have not undergone further purification prior to use. We obtained zinc acetate dihydrate (CAS 5970-45-6) and sodium hydroxide (CAS 1310-73-2)

DOI: 10.54254/2753-8818/2026.34300

from Sinopharm Chemical Reagent Co., Ltd and used them to synthesize ZnO nanoparticles. Sodium alginate (CAS# 9005-38-3) and calcium nitrate tetrahydrate (CAS# 13477-34-4), serve as the hydrogel matrix and cross-linking agent, respectively. The model dyes, Methylene Blue (CAS# 61-73-4) was also purchased from Sinopharm Chemical Reagent Co., Ltd for subsequent experiments.

3.2. Methods

3.2.1. Preparation of SA hydrogel

In order to SA hydrogel, a sodium alginate (SA) solution was prepared by dissolving 0.20 g of sodium alginate powder in 10 mL of distilled water to obtain a homogeneous and transparent 2% (w/v) solution. The mixture was placed in an oil bath and stirred continuously using a magnetic stirrer at the temperature of 65°C, and the mixture solution was stirred for 2-3 hours to promote complete dissolution of the polymer. Separately, we dissolved 2 g of NaOH in 50 mL of distilled water under continuous stirring until complete dissolution, yielding a 1 M sodium hydroxide solution. The pH of the sodium alginate solution was monitored using pH indicator strips. If the solution exhibited acidic behavior (pH < 7), the NaOH solution was added dropwise under continuous stirring. After each addition, the pH value of this mixture was measured using a fresh pH strip. This process was continued until the pH reached at approximately 7. After around 3 hours, a clear and homogeneous sodium alginate solution was obtained, indicating successful preparation. The solution was then cooled to ambient temperature and kept there for later use in hydrogel preparation.

3.2.2. Preparation of zinc oxide nanoparticle

Zinc oxide (ZnO) nanoparticles were synthesized using a hydrothermal precipitation method followed by purification and freeze-drying. First, 220 mg of zinc acetate dihydrate ($Zn(CH_3COO)_2 \cdot 2H_2O$) was weighed and then completely dissolved in 50 mL of distilled water in a beaker under continuous magnetic stirring to obtain the zinc acetate dihydrate solution. The pH of the zinc acetate solution was monitored using pH indicator strips. We added the 1M NaOH solution drop by drop to the zinc acetate solution while stirring constantly until the pH reached approximately 12. After each addition, the pH was measured using a fresh pH strip to ensure accurate adjustment. The resulting solution was transferred into a high-pressure reactor, which was then sealed and placed in an oven. The reactor was maintained at 100 °C for 1 hour to facilitate hydrothermal conversion of the precursor into ZnO nanoparticles. Once the reaction finished, we let the reactor cool to ambient temperature, then transferred the suspension into centrifuge tubes. We centrifuged the product at 12,000 rpm for 10 minutes to purify it. Then, we removed the supernatant and collected the solid precipitate.

To obtain dry ZnO nanoparticles, the collected precipitate was frozen at low temperature and subsequently subjected to freeze-drying for 48 hours. After lyophilization, a fine white powder corresponding to purified ZnO nanoparticles was obtained and stored for further characterization and use.

DOI: 10.54254/2753-8818/2026.34300

3.2.3. Preparation of zinc oxide nanoparticle embedded SA hydrogel

Dissolve 1 mg of zinc oxide nanoparticles into 1 mL of calcium nitrate tetrahydrate solution to make the ZnO nanopatile solution with Ca^{2+}. And then mix them thoroughly using a vortex mixer to obtain a zinc oxide-doped crosslinking agent solution. Subsequently, it reacts with a sodium alginate solution to embed zinc oxide within the sodium alginate matrix. After 48 hours of freeze-drying, the ZnO@SA composite hydrogel is obtained.

3.2.4. Characterization of zinc oxide nanoparticle

The morphology, structure, size, and surface chemistry of synthesized ZnO nanoparticles were systematically characterized using multiple techniques. Transmission electron microscopy (TEM) was employed to characterize morphology, dimensions, and crystal structure of nanoparticles. We further used scanning electron microscopy (SEM) to inspect the general morphology and degree of agglomeration. X-ray diffraction (XRD) analysis was conducted to characterize the crystal structure of the nanoparticles. Fourier transform infrared spectroscopy (FTIR) was applied to detect functional groups and chemical bonds on the nanoparticle surfaces.

3.2.5. Characterization of zinc oxide nanoparticle embedded SA hydrogel

To characterize the composite hydrogel, we conducted X-ray diffraction (XRD). This allowed us to examine the sodium alginate matrix's crystal structure and the changes induced by ZnO incorporation; We used Fourier transform infrared spectroscopy (FTIR) to study molecular interactions and alterations in chemical bonding inside the composite hydrogel; Scanning electron microscopy (SEM) was employed to observe the microstructure, cross-sectional morphology, and distribution of ZnO nanoparticles within the three-dimensional network of the composite hydrogel; Compression testing of the composite hydrogel was performed using a universal material testing machine to evaluate its mechanical strength and toughness; Oscillation frequency scanning tests were conducted using a rotational rheometer to determine the elastic modulus (G') and viscous modulus (G''), assessing the structural stability of the hydrogel to characterize its rheological behavior.

3.2.6. Evaluation of dye removal performance

We soaked the dry hydrogels in a methylene blue (MB) solution (1 mg/10 mL) at room temperature in the dark for a defined period. We used UV-Vis spectrophotometry to measure the dye concentration in the solution both before and after adsorption. The absorbance at the characteristic peak (λmax = 664 nm) was then recorded for quantitative analysis. Additionally, we took images to document the color change of the solution following hydrogel treatment.

4. Research analysis

4.1. Characterization of ZnO nanoparticles

4.1.1. SEM and TEM analysis of ZnO nanoparticles

The morphology and dimensions of the ZnO nanoparticles were characterized using SEM and TEM. SEM analysis (Figure 1A) shows that the ZnO nanoparticles exhibit a rectangular prism with well-

DOI: 10.54254/2753-8818/2026.34300

defined edges. Based on the SEM images, the characteristic particle size is estimated to be approximately 200 nm. Further structural characterization using TEM (Figure 1B) is consistent with the SEM observations. The TEM images reveal particles with lengths ranging from approximately 200 to 300 nm and widths between 80 and 150 nm. These results confirm the successful synthesis of ZnO nanoparticles with well-defined morphology and nanoscale dimensions.

A B

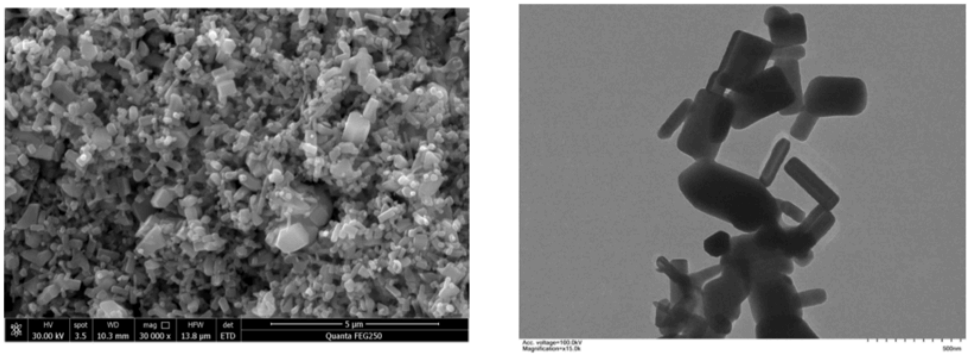

Figure 1. SEM and TEM images of ZnO nanoparticles.
A. SEM image B. TEM image

4.1.2. EDS analysis of ZnO nanoparticles

We performed Energy Dispersive Spectroscopy (EDS) to identify the elemental makeup of the as-prepared material. The EDS spectrum (Figure 2A) shows prominent peaks corresponding to zinc (Zn) and oxygen (O), confirming that the prepared nanoparticle is composed of Zinc and Oxygen. A strong oxygen peak is observed at low energy (~0.5 keV), consistent with the presence of oxide species. Distinct zinc peaks are detected at approximately 8.6 keV (Zn K_{α}) and 9.6 keV (Zn K_{β}), which are characteristic of elemental zinc. No significant peaks corresponding to other metallic or non-metallic elements were detected, suggesting minimal impurity incorporation and high material purity.

A B

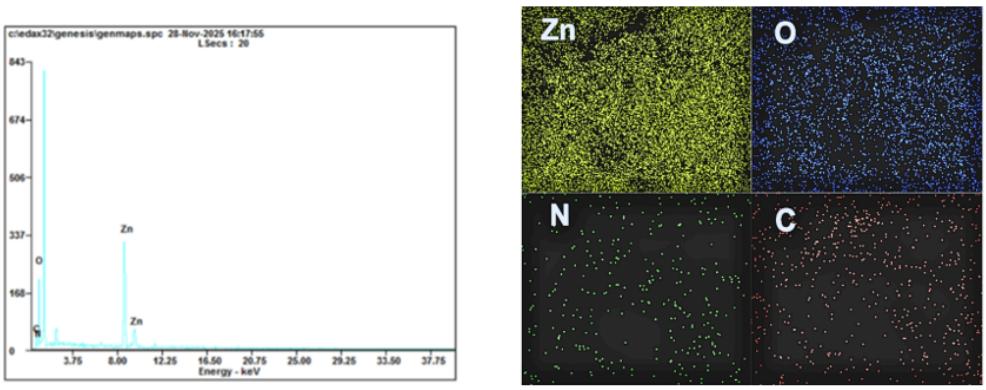

Figure 2. EDS analysis of ZnO nanoparticles
A. EDS spectrum B. EDS elemental mapping

DOI: 10.54254/2753-8818/2026.34300

Elemental distribution within the synthesized material was further examined using EDS elemental mapping (Figure 2B). The mapping images show a uniform and homogeneous distribution of zinc (Zn) in yellow and oxygen (O) in blue across the analyzed region, indicating consistent composition throughout the nanoparticle. The Zn elemental map exhibits a dense and evenly dispersed signal, confirming that zinc is distributed within the whole nanoparticle. Similarly, the oxygen map shows a widespread distribution that spatially overlaps with zinc, further supporting the formation of zinc oxide (ZnO). The analysis also detected weak signals from carbon (C) and nitrogen (N). These elements are attributed to the raw chemical of Zinc acetate, rather than impurities in the ZnO phase.

4.1.3. XRD analysis of ZnO nanoparticles

We conducted X-ray diffraction (XRD) to examine the crystal structure and phase makeup of the prepared material. The XRD pattern (Figure 3A) exhibits a series of sharp and well-defined diffraction peaks, indicating a highly crystalline structure. The prominent diffraction peaks observed at approximately 31.7°, 34.4°, and 36.2° (2θ) correspond to the (100), (002), and (101) crystal planes zinc oxide (ZnO), respectively. Additional peaks appearing at higher angles (around 47.5°, 56.6°, 62.8°, and above) further match the standard diffraction pattern of ZnO (JCPDS No. 36-1451 [15]), confirming the successful formation of crystalline ZnO. No extra peaks associated with secondary phases or impurities are detected, suggesting high phase purity of the synthesized ZnO. The sharpness and intensity of the diffraction peaks further indicate good crystallinity, which is beneficial for adsorption and photocatalytic applications.

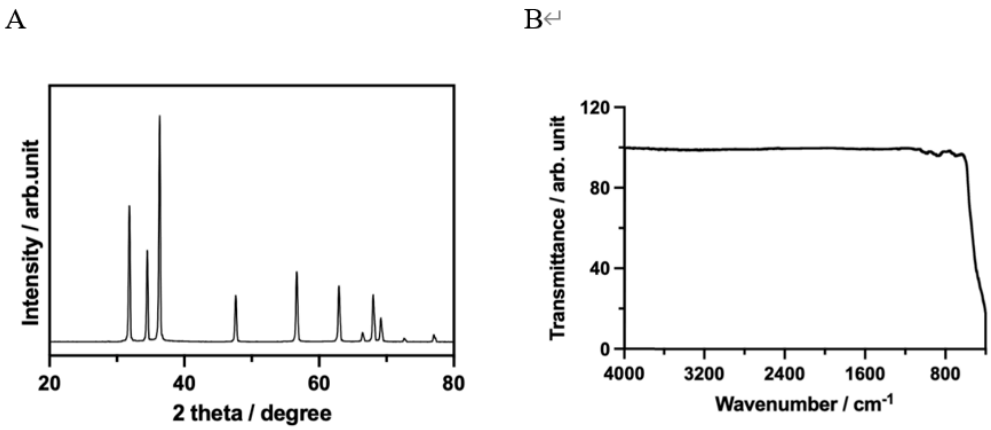

Figure 3. XRD pattern and FTIR spectrum of ZnO nanoparticles

4.1.4. FTIR analysis of ZnO nanoparticles

We employed Fourier Transform Infrared (FTIR) spectroscopy to detect the functional groups and chemical bonds existing in the prepared nanoparticles. The FTIR spectrum (Figure 3B) shows a largely flat transmittance profile across the mid-infrared region, indicating minimal organic functional group contributions. We assign the intense absorption band appearing below ~ 800 cm^{-1} to Zn-O stretching vibrations, which confirms the existence of zinc oxide bonds. The absence of pronounced peaks in the regions corresponding to O-H (3200-3600 cm^{-1}), C-H (2800-3000 cm^{-1}), and C=O (around 1700 cm^{-1}) stretching vibrations suggests that raw chemical residues are minimal. The lack of strong organic absorption bands indicates effective formation of inorganic ZnO and limited

DOI: 10.54254/2753-8818/2026.34300

interference from residual precursor compounds.The results in figure 4.4 support the successful formation of ZnO nanoparticles in lengths and widths.

4.2. Characterization of the ZnO nanoparticle-embedded hydrogel

4.2.1. Preparation of ZnO@SA hydrogel

Following the described procedure, the ZnO nanoparticle-embedded hydrogel was successfully formed (Figure 4A). The material confirms the transition from a liquid solution to a crosslinked hydrogel network.

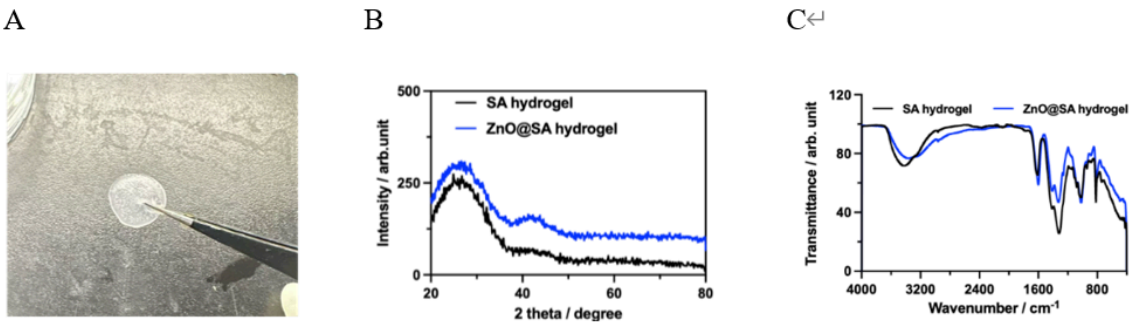

Figure 4. Morphology, XRD and FTIR characterization of ZnO nanoparticle-embedded SA hydrogel (A) Hydrogel image; (B) XRD patterns of SA and ZnO@SA hydrogel; (C) FTIR spectrum of SA and ZnO@SA hydrogel

4.2.2. XRD analysis

X-ray diffraction (XRD) patterns of the freeze-dried sodium alginate (SA) hydrogel and ZnO nanoparticle-embedded SA hydrogel are shown in Figure 4B. For the control SA hydrogel, a broad diffraction peak appears near 20-30°, which is typical for an amorphous polymeric material. By comparison, the ZnO@SA hydrogel shows stronger diffraction intensity along with extra broad features, revealing that ZnO nanoparticles have been successfully introduced into the hydrogel network. Moreover, no sharp crystalline peaks are observed, implying that the ZnO nanoparticles are evenly dispersed and remain embedded inside the amorphous alginate matrix instead of aggregating into large crystals.

4.2.3. FTIR analysis

FTIR spectra of the freeze-dried SA hydrogel and ZnO@SA hydrogel are shown in Figure 4C. Both samples exhibit a broad absorption band around 3200-3400 cm^{-1}, corresponding to O-H stretching vibrations of hydroxyl groups in the alginate backbone and absorbed water. We assign the bands at approximately 1600 cm^{-1} and 1400 cm^{-1} to the asymmetric and symmetric stretching modes of carboxylate ($-COO^-$) groups, which are typical for sodium alginate. When compared to the control SA hydrogel, the ZnO@SA hydrogel exhibits clear differences in peak intensity and minor peak shifts within the carboxylate region, suggesting that ZnO nanoparticles interact with the alginate matrix. These changes suggest coordination or electrostatic interactions between Zn^{2+} sites on ZnO and alginate functional groups, confirming successful incorporation of ZnO nanoparticles into the hydrogel network without altering the fundamental chemical structure of SA.

DOI: 10.54254/2753-8818/2026.34300

4.2.4. Rheological analysis

As shown in Figure 5A, the storage modulus (G') exceeds the loss modulus (G") throughout the measured range, indicating an elastic-dominated response. Beyond confirming gel formation, the stable separation between G' and G" suggests a mechanically robust network with sufficient crosslink density to resist structural breakdown under shear.

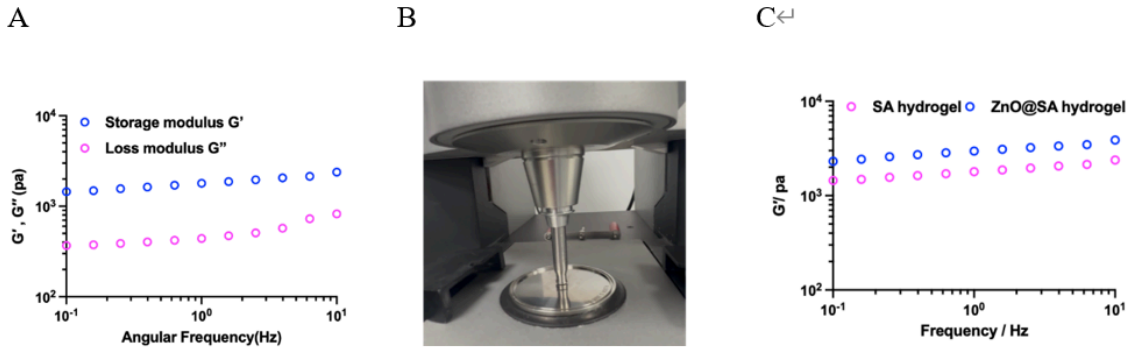

Figure 5. Rheological analysis of SA and ZnO@SA hydrogels
(A) Frequency sweeps analysis of SA hydrogel; (B) Photograph of the rheometer; (C) Storage modulus of SA and ZnO@SA hydrogel

4.2.5. Rheological analysis

Rheological measurements were performed using a rotational rheometer (Figure 5B) to evaluate the viscoelastic properties of the SA hydrogel and ZnO@SA hydrogel. We employed a rheometer to determine the storage modulus (G'), which reflects elastic behavior, and the loss modulus (G"), which reflects viscous behavior.

This behavior was further compared through frequency-sweep rheological measurements of the SA hydrogel and ZnO@SA hydrogel (Figure 5C). Across the tested frequency range, both materials exhibit relatively weak frequency dependence, indicating stable viscoelastic networks. Notably, the ZnO@SA hydrogel consistently shows higher modulus values than the control SA hydrogel, reflecting increased network stiffness resulting from ZnO nanoparticle incorporation.

4.2.6. SEM analysis

Scanning electron microscopy (SEM) images of the freeze-dried SA hydrogel and ZnO@SA hydrogel are shown in Figures 6A and B, respectively. The control SA hydrogel exhibits a highly porous, interconnected three-dimensional network with relatively large and irregular pore structures, characteristic of ionically crosslinked alginate hydrogels. The pore size is on average 200 μm. In contrast, the ZnO@SA hydrogel displays a visibly denser microstructure with reduced pore size and thicker pore walls. Discrete nanoscale features distributed along the polymer matrix are observed in the ZnO@SA hydrogel, which are attributed to embedded ZnO nanoparticles. The pore size is reduced to on average 150 μm. The reduction in pore size and increased structural compactness suggest that ZnO nanoparticles act as physical fillers or additional interaction sites within the alginate network, leading to partial pore contraction and enhanced network reinforcement.

DOI: 10.54254/2753-8818/2026.34300

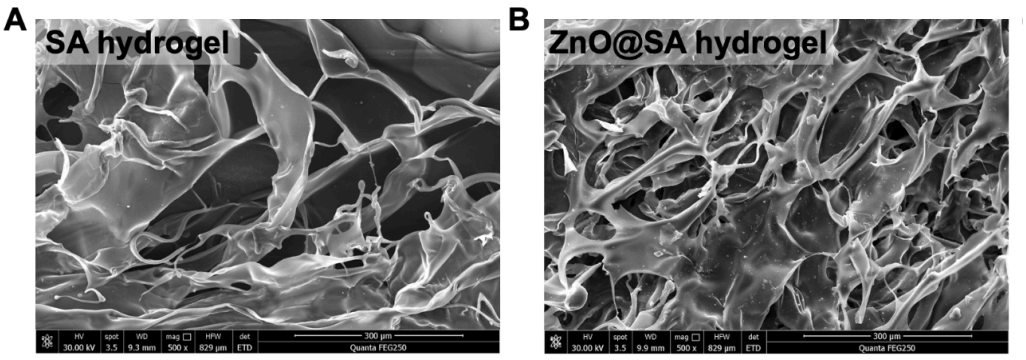

Figure 6. SEM image of SA hydrogel and ZnO@SA hydrogel
A.SA hydrogel B. ZnO@SA hydrogel

4.2.7. EDS analysis

Energy-dispersive X-ray spectroscopy (EDS) was used to analyze the elemental composition of the SA hydrogel and ZnO@SA hydrogel, as shown in Figures 7A an B. The spectrum of the control SA hydrogel is dominated by carbon and oxygen signals, consistent with the alginate polymer matrix, with a low zinc content of 0.72 wt%, attributed to background signal or trace contamination. In contrast, the ZnO@SA hydrogel exhibits a pronounced Zn signal, with the zinc content increasing to 1.92 wt%, confirming successful incorporation of ZnO nanoparticles within the hydrogel matrix. The rise in Zn content, along with the preserved C and O signals, suggests that ZnO nanoparticles are incorporated into the alginate network instead of substituting the polymer framework.

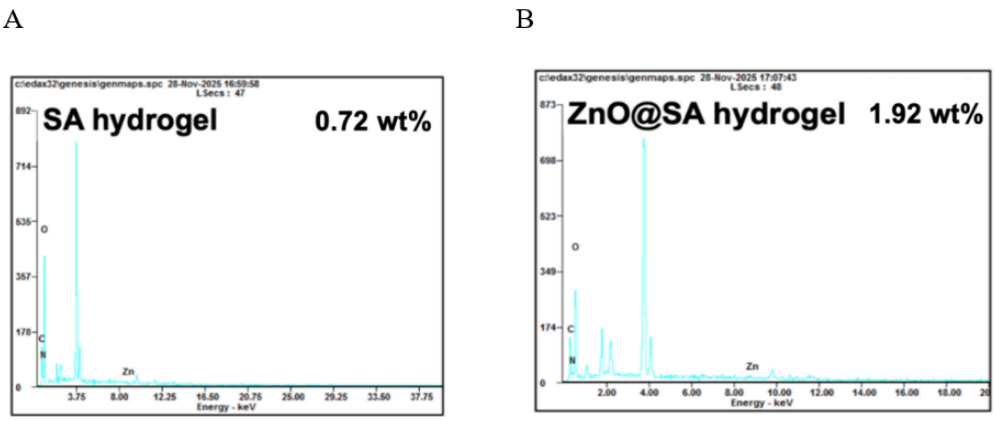

Figure 7. Corresponding EDS of SA hydrogel and ZnO@SA hydrogel
A. SA hydrogel B. ZnO@SA hydrogel

4.2.8. Tensile mechanical properties analysis

Mechanical testing using the Universal Material Testing Machine was conducted to compare the mechanical behavior of the SA hydrogel and ZnO@SA hydrogel Figure 8A. The corresponding stress–strain curves are shown in Figure 8B. The control SA hydrogel exhibits a higher peak stress prior to failure, indicating greater tensile strength compared to the ZnO@SA hydrogel. In contrast, the ZnO@SA hydrogel displays a lower maximum stress but a more gradual stress increase, suggesting altered stress distribution within the polymer network following ZnO incorporation. This

DOI: 10.54254/2753-8818/2026.34300

behavior indicates that while ZnO nanoparticles reinforce the hydrogel at small deformations, they may introduce localized stress concentration or network heterogeneity that limits ultimate tensile strength. The above results indicate that the stable ZnO@ SA hydrogel with the pore size of 100 μm can be successfully obtained.

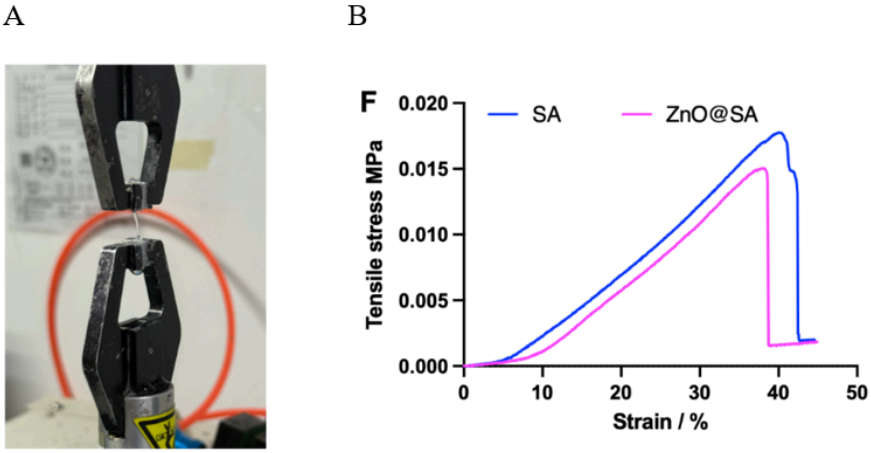

Figure 8. Mechanical property testing of hydrogels
(A) Photograph of the universal material testing machine; (B) Tensile mechanical properties of SA and ZnO@SA hydrogel

4.3. Charcterization of dye adsorption properties

4.3.1. Adsorption performance of ZnO@SA hydrogel for methylene blue

The methylene blue(MB) adsorption performance of the control SA hydrogel and ZnO@SA hydrogel is visually compared in Figure 9. The left three samples correspond to the SA hydrogel, while the remaining samples contain the ZnO@SA hydrogel.

After exposure to methylene blue solution, the SA hydrogel samples show partial decolorization of the supernatant, indicating dye adsorption by the alginate matrix. However, noticeable blue coloration remains in the solution, suggesting limited adsorption capacity. In contrast, the ZnO@SA hydrogel samples exhibit significantly greater decolorization of the surrounding solution, accompanied by more intense blue coloration within the hydrogel phase. This indicates enhanced uptake of methylene blue by the ZnO-embedded hydrogel.

DOI: 10.54254/2753-8818/2026.34300

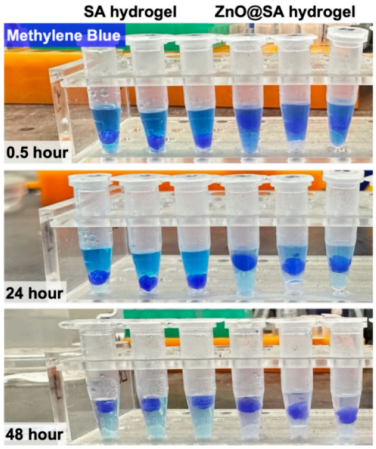

Figure 9. Photo comparison of methylene blue in hydrogel treatment with time

4.3.2. Quantitative analysis of ZnO@SA hydrogel removal performance for methylene blue

UV–Vis spectroscopy was used to compare the methylene blue removal performance of the SA hydrogel and ZnO@SA hydrogel by monitoring the characteristic absorption peak at 665 nm (Figure 10A). After treatment, both samples show a decrease in absorbance intensity, indicating successful adsorption of methylene blue from solution. Notably, the ZnO@SA hydrogel exhibits a significantly greater reduction in the 665 nm absorbance compared to the SA hydrogel under identical conditions, indicating a lower residual dye concentration. This result demonstrates that incorporation of ZnO nanoparticles enhances the dye adsorption capacity of the alginate hydrogel, consistent with the visual decolorization observations.

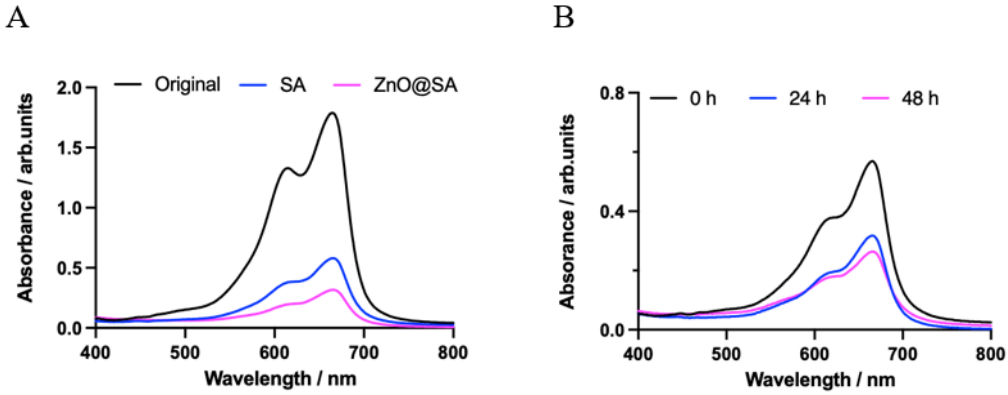

Figure 10. UV-vis absorption spectrum of MB solutions
(A) Original MB solution, SA hydrogel and ZnO@SA hydrogel after 48 h; (B) MB solution after treatment with ZnO@SA hydrogel across 48 h

4.3.3. Sustained adsorption performance of ZnO@SA hydrogel

The time-dependent adsorption performance of the ZnO@SA hydrogel was further evaluated by UV-Vis spectroscopy over multiple days (Figure 10B). A progressive decrease in absorbance at 665 nm is observed from 0 h to 48 h, indicating continuous removal of methylene blue from solution over time. The gradual attenuation of the absorption peak suggests sustained adsorption activity of the ZnO@SA hydrogel, demonstrating its ability to maintain dye uptake beyond the initial contact

DOI: 10.54254/2753-8818/2026.34300

period. This time-dependent behavior indicates that the hydrogel possesses sufficient adsorption capacity and structural stability for prolonged operation.

The results above indicate that the ZnO@SA hydrogel exhibits superior adsorption capability compared to the control SA hydrogel. This enhancement is attributed to the incorporation of ZnO nanoparticles, which introduce additional adsorption sites within the alginate matrix. Furthermore, ZnO incorporation leads to a reduction in pore size, increasing the effective surface area and facilitating stronger interactions between the hydrogel and dye molecules, thereby further improving adsorption performance.

5. Discussion and conclusion

In this study, zinc oxide nanoparticles with lengths of 200-300 nm and widths of 80-150 nm were successfully synthesized. We mixed these nanoparticles into a sodium alginate (SA) solution, resulting in a stable ZnO@SA hydrogel whose average pore size was about 100 μm. The prepared ZnO@SA hydrogel exhibited superior adsorption performance for methylene blue removal compared to the control SA hydrogel after 48 h of treatment. The enhanced adsorption capability is attributed to the introduction of nanosized ZnO particles, which provide additional adsorption sites within the hydrogel matrix. Furthermore, ZnO incorporation reduces the pore size of the hydrogel, increasing effective surface area and facilitating stronger dye-hydrogel interactions, thereby further improving adsorption efficiency.

The ZnO@SA composite hydrogel developed in this study offers an efficient and economical solution for dye-contaminated wastewater treatment. This composite hydrogel not only demonstrates outstanding adsorption performance and structural stability, but its biocompatible sodium alginate matrix combined with a nano-reinforcement strategy also provides valuable insight into the design of environmentally friendly and scalable adsorbents. Beyond laboratory performance, the material will demonstrate strong potential for real-world application. If adopted in global textile wastewater treatment, it would significantly increase the proportion of safely treated water. This advancement would contribute to progress toward the UN Sustainable Development Goal (SDG) for safe wastewater treatment, helping to push global efforts closer to the 2030 target. Future work can further optimize the hydrogel's composition and structure to expand its application in the synergistic removal of multiple pollutants and in practical, large-scale water purification systems.

References

[1] Lin, J., Ye, W., Xie, M., Seo, D. H., Luo, J., Wan, Y., & Van der Bruggen, B. (2023). Environmental impacts and remediation of dye-containing wastewater. Nature Reviews Earth & Environment, 4(11), 785-803.

[2] Hu, X. S., Liang, R., & Sun, G. (2018). Super-adsorbent hydrogel for removal of methylene blue dye from aqueous solution. Journal of Materials Chemistry A, 6(36), 17612-17624.

[3] Shalla, A. H., Bhat, M. A., & Yaseen, Z. (2018). Hydrogels for removal of recalcitrant organic dyes: A conceptual overview. Journal of environmental chemical engineering, 6(5), 5938-5949.

[4] Jung, S., Yun, H., Kim, J., Kim, J., Yeo, H., Choi, I. G., & Kwak, H. W. (2024). Lignin/PVA hydrogel with enhanced structural stability for cationic dye removal. International Journal of Biological Macromolecules, 257, 128810.

[5] Gao, X., Guo, C., Hao, J., Zhao, Z., Long, H., & Li, M. (2020). Adsorption of heavy metal ions by sodium alginate based adsorbent-a review and new perspectives. International journal of biological macromolecules, 164, 4423-4434.

[6] Verma, A., Thakur, S., Mamba, G., Gupta, R. K., Thakur, P., & Thakur, V. K. (2020). Graphite modified sodium alginate hydrogel composite for efficient removal of malachite green dye. International Journal of Biological Macromolecules, 148, 1130-1139.

DOI: 10.54254/2753-8818/2026.34300

[7] Alraddadi, H. M., Fagieh, T. M., Bakhsh, E. M., Akhtar, K., Khan, S. B., Khan, S. A., ... & Homdi, T. A. (2023). Adsorptive removal of heavy metals and organic dyes by sodium alginate/coffee waste composite hydrogel. International Journal of Biological Macromolecules, 247, 125708.
[8] Lai, W., Zhang, L., Liang, Y., Zhang, G., Zou, J., & Fei, P. (2025). Carboxyethyl chitosan/oxidized sodium alginate composite hydrogel loaded with AgNPs and Zn2+: dye adsorption and antibacterial function. International Journal of Biological Macromolecules, 309, 143124.
[9] Hussain, S., Salman, M., Youngblood, J. P., Farooq, U., Yasmeen, S., Al-Ahmary, K. M., & Ahmed, M. (2024). Enhanced adsorption of Congo red dye by CS/PEG/ZnO composite hydrogel: Synthesis, characterization, and performance evaluation. Journal of Molecular Liquids, 411, 125704.
[10] Zhou, C., Wang, C., Xu, K., Niu, Z., Zou, S., Zhang, D., ... & Xie, J. (2023). Hydrogel platform with tunable stiffness based on magnetic nanoparticles cross-linked GelMA for cartilage regeneration and its intrinsic biomechanism. Bioactive Materials, 25, 615-628.
[11] Qian, J., Gao, X., & Pan, B. (2020). Nanoconfinement-mediated water treatment: from fundamental to application. Environmental Science & Technology, 54(14), 8509-8526.
[12] Sayyar, Z., Hosseini, Z., Pakdel, P. M., & Hassani, A. (2024). Preparation of novel and low-cost chitosan modified with montmorillonite/ZnO hydrogel nanocomposite for adsorption of ciprofloxacin from water. Journal of Water Process Engineering, 63, 105449.
[13] Puneetha, J., Kottam, N., & Rathna, A. (2021). Investigation of photocatalytic degradation of crystal violet and its correlation with bandgap in ZnO and ZnO/GO nanohybrid. Inorganic Chemistry Communications, 125, 108460.
[14] Asjadi, F., & Yaghoobi, M. (2022). Characterization and dye removal capacity of green hydrothermal synthesized ZnO nanoparticles. Ceramics International, 48(18), 27027-27038.
[15] Xu, F., Mei, W., Hu, P., Zheng, L., Zhang, J., Cao, H., ... & Yu, J. (2025). Spatially Engineered Ternary Schottky/S-Scheme Heterojunctions for Artificial Photosynthesis. Angewandte Chemie International Edition, 64(39), e202513364.